Analyzing Gaps in Hurricane Rain Coverage to Inform Future Satellite Proposals

Justin Stow[1,2]

Committee: Mark A. Bourassa[1,2], Heather Holbach[2,4], Vasubandhu Misra[1,2], Monica Hurdal[3]

IOVWST Meetng

[1]Department of Earth, Ocean, and Atmospheric Sciences, Florida State University, Tallahassee, FL

[2]Center for Ocean-Atmospheric Prediction Studies, 2000 Levy Ave., Building A, Suite 292, Tallahassee, FL

[3]Department of Mathematics, Florida State University, Tallahassee, FL

[4]Hurricane Research Division, Miami, FL

Motivation

- Remote sensing has become an increasingly popular way to estimate properties of various meteorological and oceanographic phenomena (precipitation, SSTs, surface winds, ocean currents)
- Accurate tropical cyclone (TC) forecasting requires high-resolution surface observations from operational aircraft and satellites
- Determine if already proposed satellite mission can be used for this application
- Distribution of gap sizes in moderate to heavy rainbands that circulate around the main low pressure center has not been studied in this context

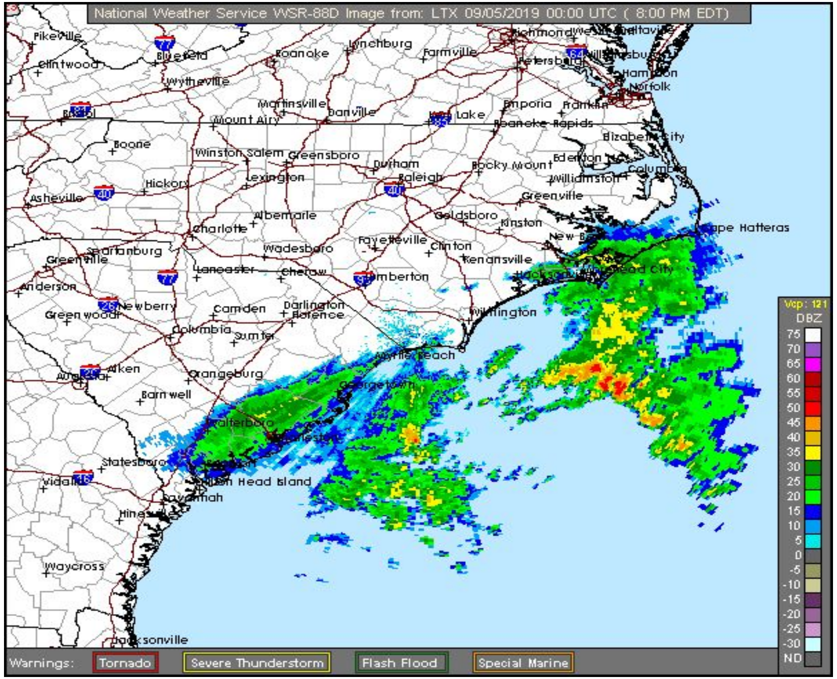

Hurricane Dorian (2019) Reflectivity Data approaching Carolina coast (National Weather Service 2019)

Satellite Mission Concept

- National Academies of Sciences, Engineering, and Medicine (2018) highly recommends future NASA Earth Explorer missions

- One such mission is a satellite to measure high resolution surface winds and currents

- There are a range of instrument design options that could be used to achieve the main scientific goals
    - Resolution
    - Accuracy
    - Coverage

The National Academies of
SCIENCES · ENGINEERING · MEDICINE

Winds and Currents Mission

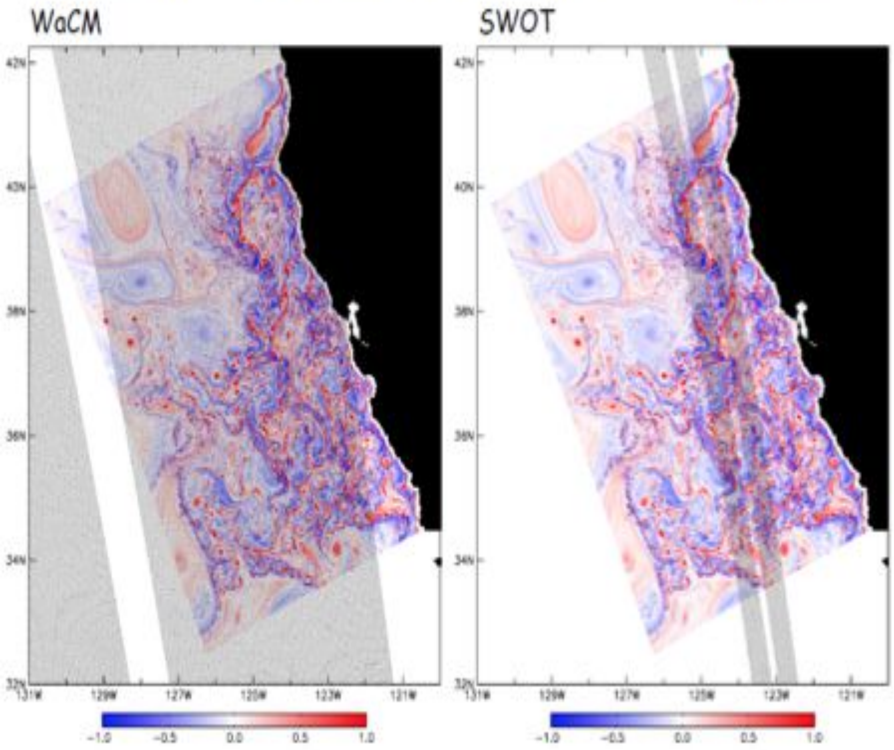

Comparison of WaCM and SWOT Measurement Swaths
(Bourassa and others 2019, Chelton et al. 2019)

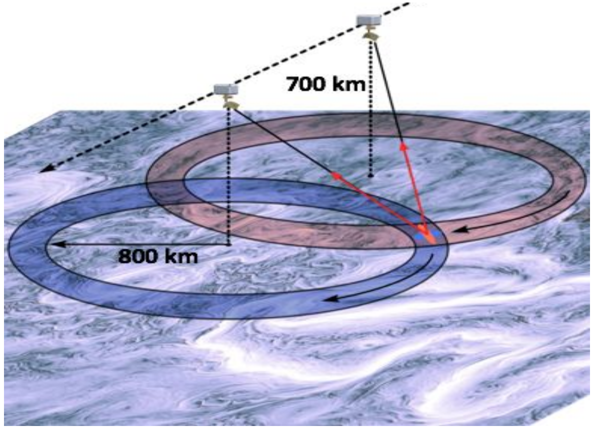

WaCM Measurement Concept - pencil-beam Doppler scatterometers measuring winds from Ka or Ka/Ku sigma signals at multiple azimuth angles (Bourassa and others 2019)

- Rodriguez et al. (2019) demonstrated WaCM measures ocean winds and surface currents accurately
- Winds: observed by radars
- Currents: police radar gun method (speed of ripples)
- Wide swath & fast sampling = less aliasing of time-averaged currents and derivatives
  - Mitigate noisier single-pass measurements

Objectives

Determine instrument design characteristics that allow the satellite concept mission (e.g. Winds and Currents Mission (WaCM) & Sea surface KInematics Multiscale monitoring (SKIM)) to offer knowledge of surface under tropical cyclones (ocean vector winds, oceanic surface currents, waves, etc.).

These characteristics depend on knowledge of:

a. Rainband gaps (areas *through* which a satellite can see surface)
b. How these gaps change depending on type of storm

Data Used: NOAA Aircraft Radar

- Aircraft: NOAA's WP-3D Turboprop (N42RF, N43RF)
- Radar: Lower Fuselage (LF)
- LF radar system changed in 2018, using old system here
- Calculations in plane-relative coordinates
- HRD's MATLAB function converted to Python for plotting and numerical calculations
- Benefits:
  - Data availability
  - Resolution
  - Spatial coverage

WP-3D N42RF NOAA aircraft containing flight-level data sensors, airborne radars, remote sensors, and cloud physics instrumentation (HRD 2014)

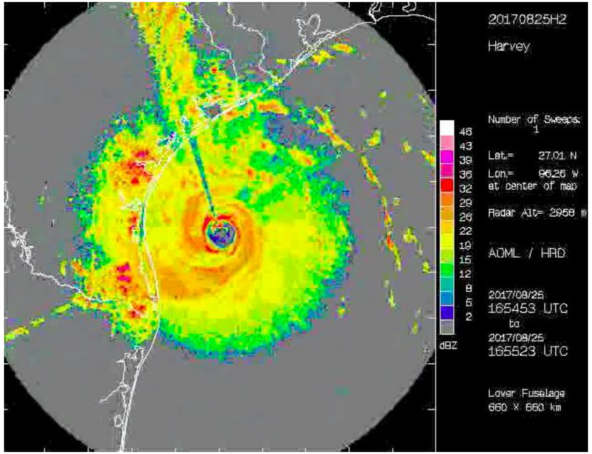

Single Lower Fuselage Sweep of Hurricane Harvey (HRD 2018)

Estimating Rain Rates

- Simple rainrate used as proxy for columnar integrated rain rate
- Assumed constant height column reflectivity up to freezing level
  - Verified by HRD Tail Doppler (TDR) imagery
- LF radar measures in reflectivity (dBz) of clouds/precipitation
- Applied Marshall-Palmer conversion formula based on commonality and easy computation
- Apply chosen thresholds to computed rates to determine rain-free regions

Marshall-Palmer Conversion Formula

(Marshall, Langille, and Palmer 1947)

$$RR = \left(\frac{10^{(dbz/10)}}{200}\right)^{0.625}$$

Case Study Selection

- Ignore viewing angle ("looking straight down")
- Selected input parameters to test:
  - Footprint Sizes: 1.375, 2.75, 4.125, 5.5 km
    - Viewing Areas: 2.75, 5.5, 8.25, 11 km
  - Rainrate Thresholds: 0.1 - 10.0 mm/hr (Draper and Long 2004)
- Incorporated storms with varying environmental stresses (wind shear, moisture influx, dry air intrusions)
- Rationale:
  - *Harvey*: rapid intensification, slight land interference, radiofrequency interference
  - *Irma, **Maria***: symmetric, weak vertical wind shear, large/strong storms
  - ***Jose**, Nate*: antisymmetric, strong vertical wind shear, relatively smaller/weaker storms

CASE STUDIES

Storm	Date, Time (UTC)	Vmax (mph)
AL092017 Harvey	Aug. 25th, 2017 16:54:53	112
AL112017 Irma	Sept. 5th, 2017 9:45	171
AL122017 Jose	**Sept. 18th, 2017 1:57:11**	**92**
AL142017 Maria	**Sept. 24th, 2017 8:14:29**	**94**
AL152017 Nate	Oct. 7th, 2017 10:48:44	82

Viewing Area Structures

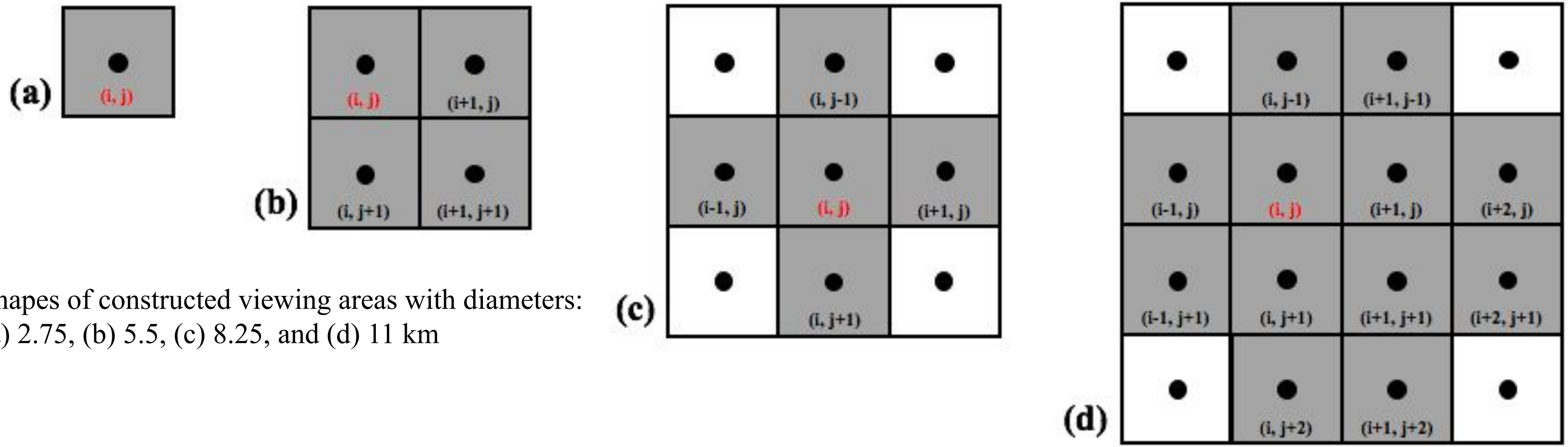

Shapes of constructed viewing areas with diameters:
(a) 2.75, (b) 5.5, (c) 8.25, and (d) 11 km

- Coarse resolution prevents perfect circular shape
- Loop through each radar sweep to determine rainfree areas & observable areas
- Ensured each part of footprint remained on radar sweep & rain-free

Maria (AL152017)

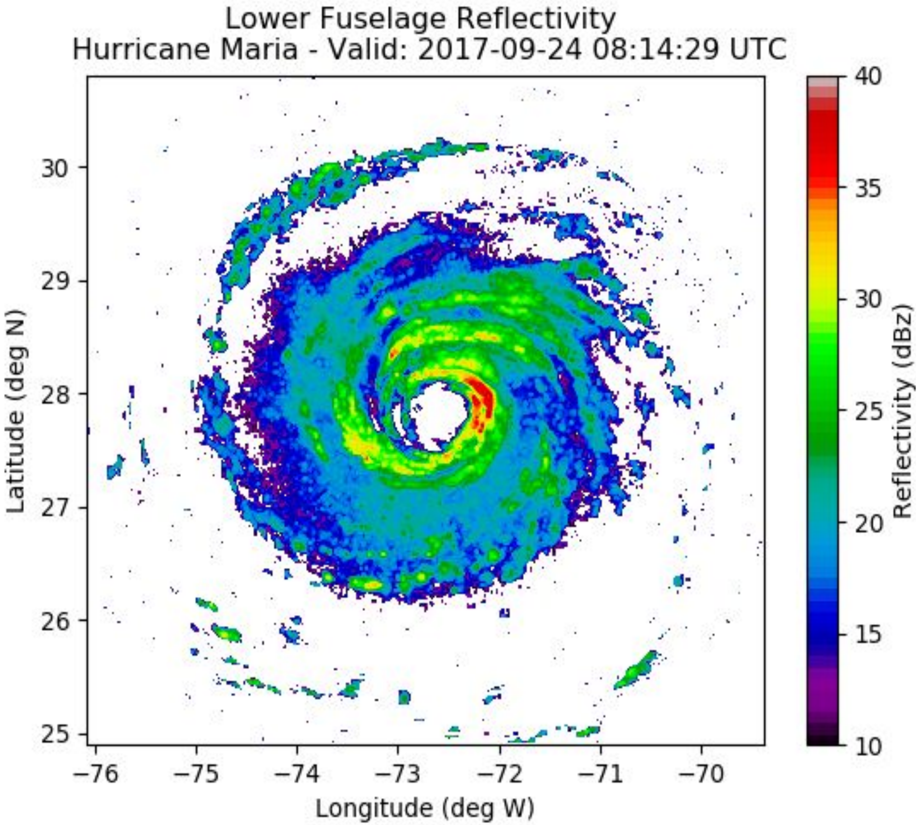

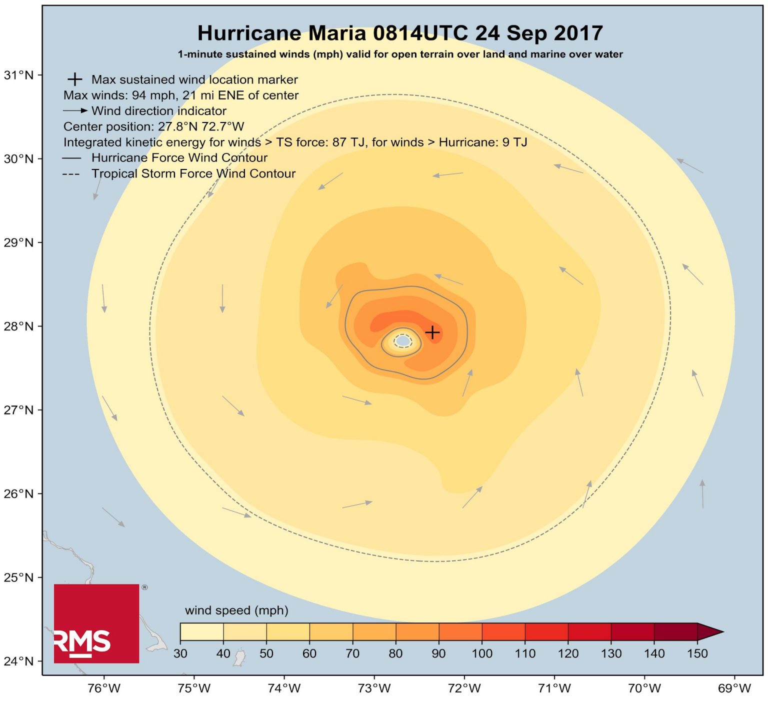

0.1 mm/hr Threshold (Ka-Band)

2.75 km Footprint

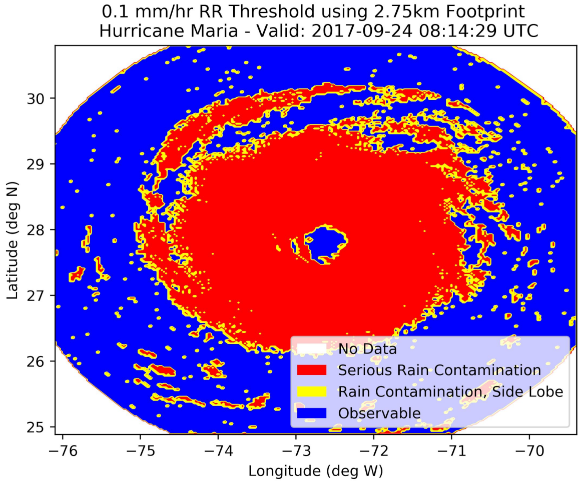

4.125 km Footprint

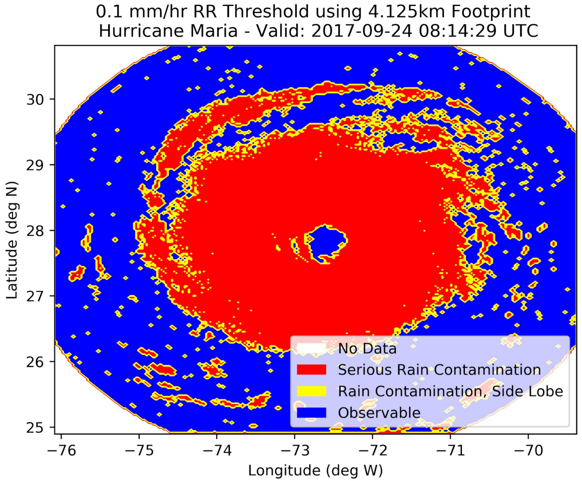

5.5 km Footprint

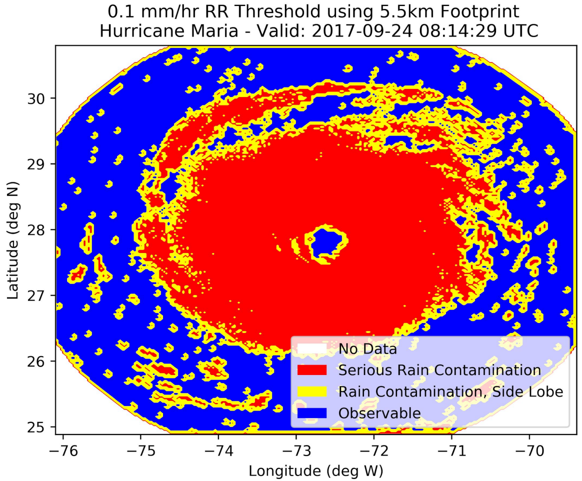

0.1 mm / hr rainrate threshold applied to reflectivity data for Maria (September 24th, 2017 8:14:29 UTC) with three shades:
blue: rainrate threshold met *and* surface observable
yellow: rainrate threshold met but surface *not* observable,
red: rainrate threshold not met *and* surface not observable

0.6 mm/hr Threshold (Ku-Band)

2.75 km Footprint

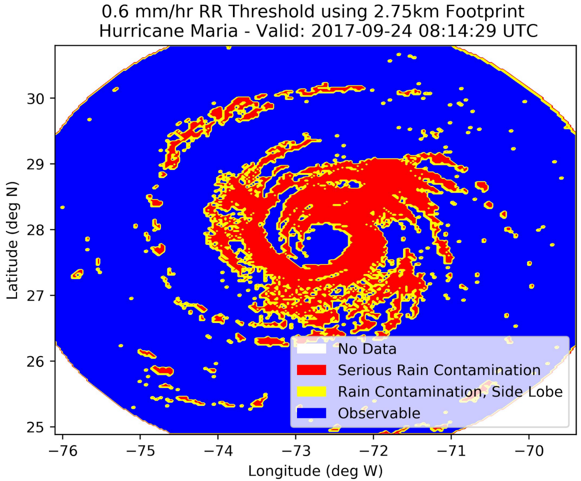

4.125 km Footprint

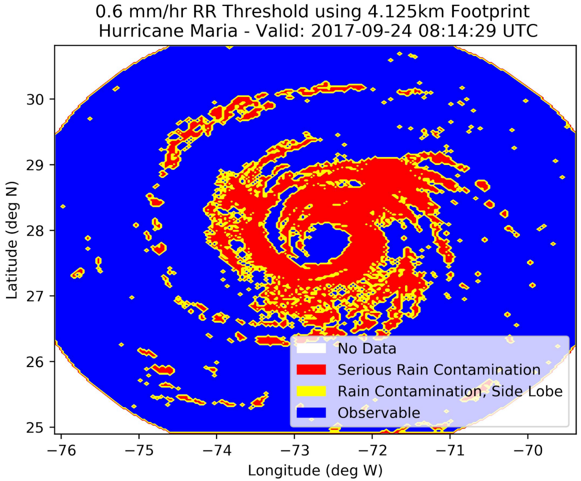

5.5 km Footprint

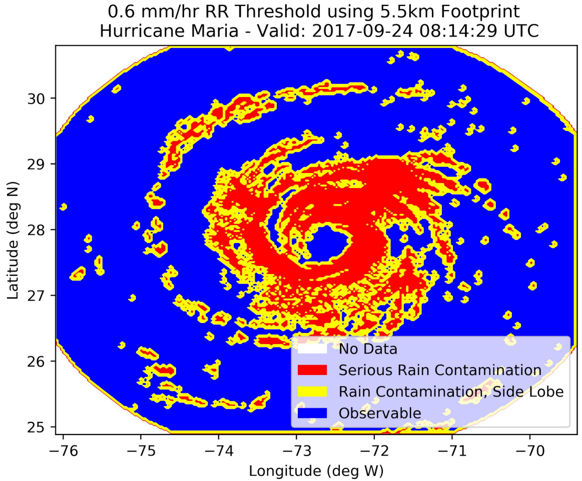

0.6 mm / hr rainrate threshold applied to reflectivity data for Maria (September 24th, 2017 8:14:29 UTC) with three shades:
blue: rainrate threshold met *and* surface observable
yellow: rainrate threshold met but surface *not* observable,
red: rainrate threshold not met *and* surface not observable

8.0 mm/hr Threshold (C-Band)

2.75 km Footprint

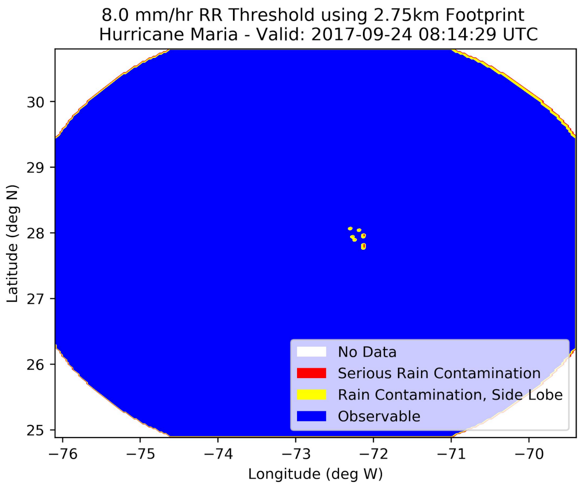

4.125 km Footprint

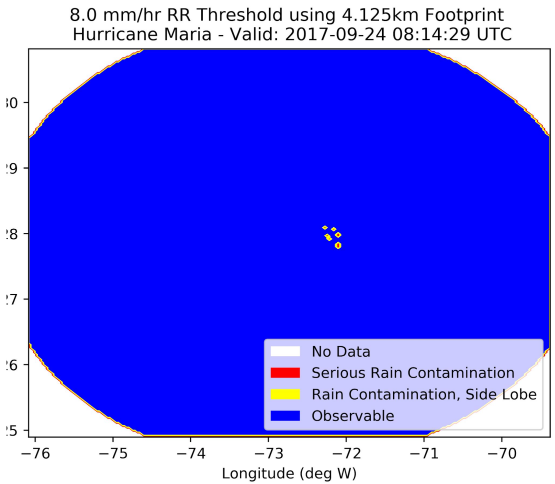

5.5 km Footprint

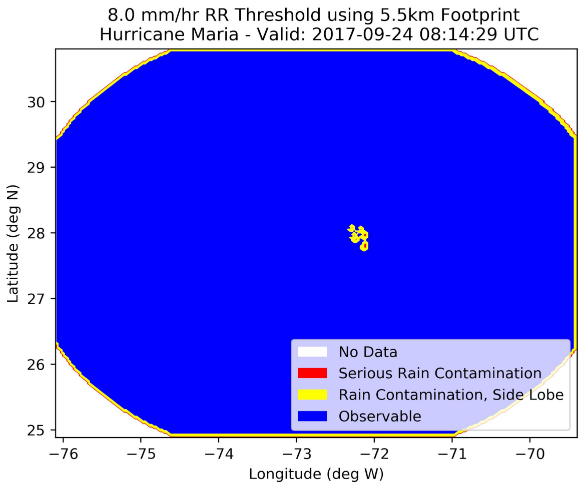

8.0 mm / hr rainrate threshold applied to reflectivity data for Maria (September 24th, 2017 8:14:29 UTC) with three shades:

blue: rainrate threshold met *and* surface observable

yellow: rainrate threshold met but surface *not* observable,

red: rainrate threshold not met *and* surface not observable

Jose (AL122017)

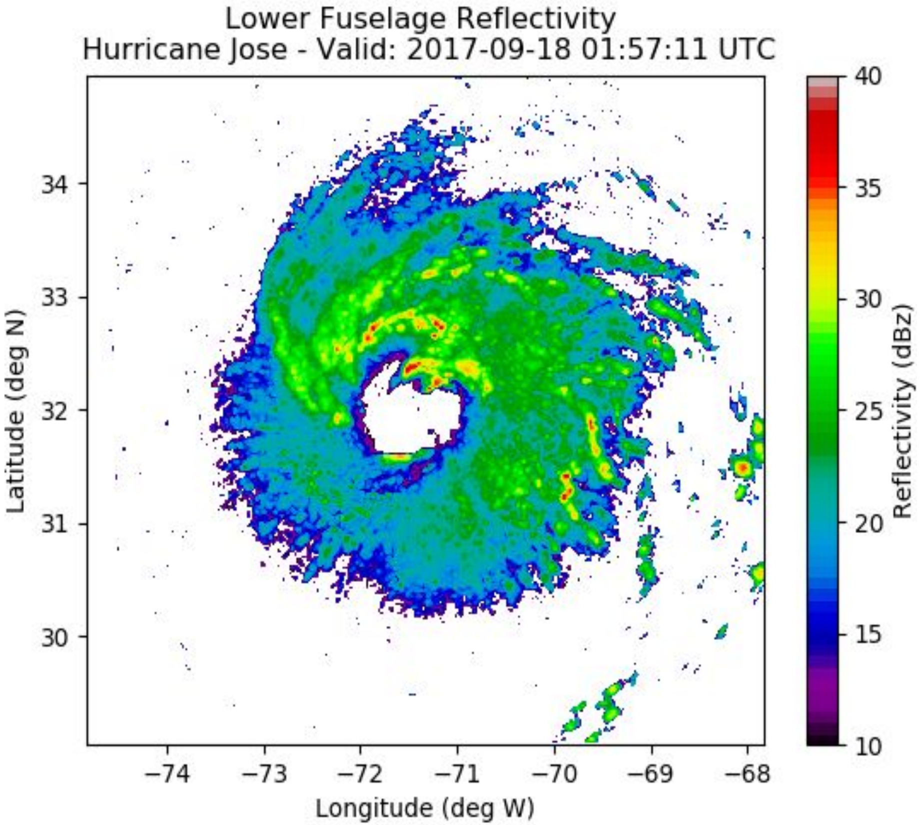

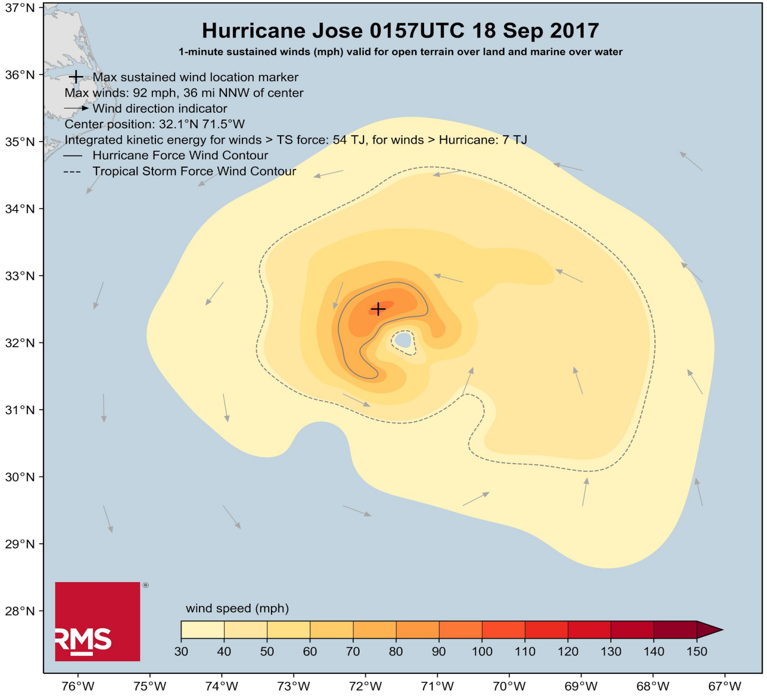

0.1 mm/hr Threshold (Ka-Band)

2.75 km Footprint

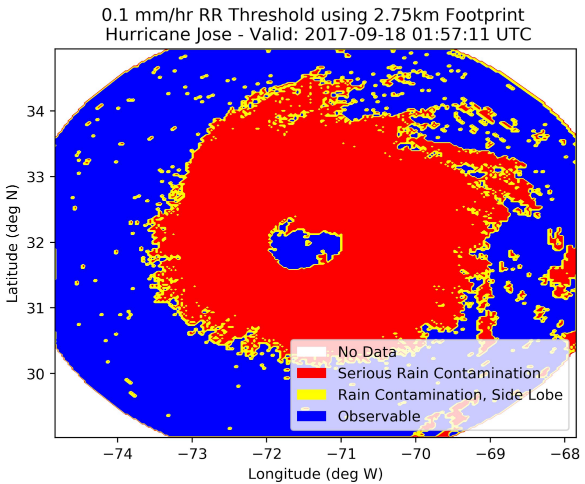

4.125 km Footprint

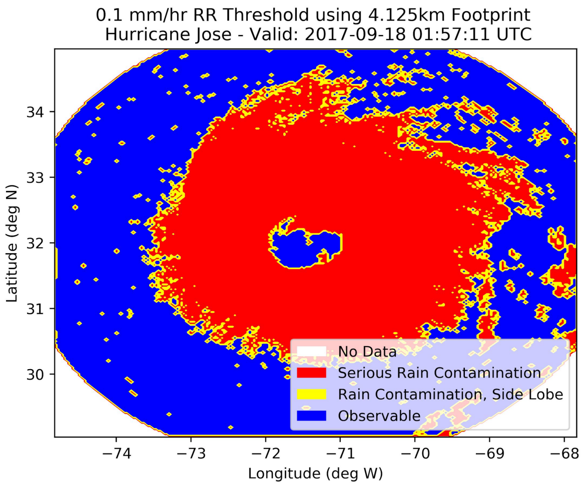

5.5 km Footprint

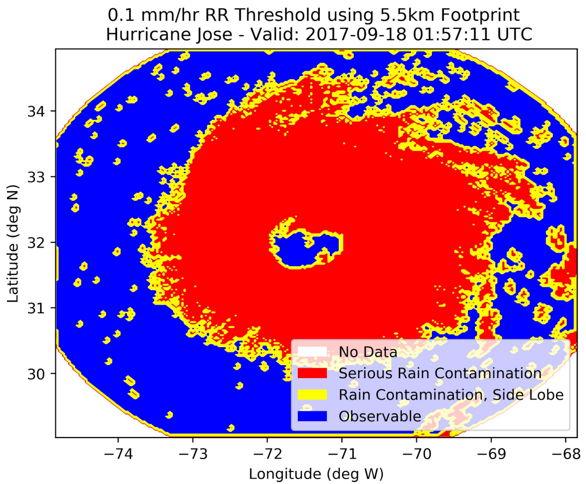

0.1 mm / hr rainrate threshold applied to reflectivity data for Jose (September 18th, 2017 1:57:11 UTC) with three shades:
blue: rainrate threshold met *and* surface observable
yellow: rainrate threshold met but surface *not* observable,
red: rainrate threshold not met *and* surface not observable

0.6 mm/hr Threshold (Ku-Band)

2.75 km Footprint

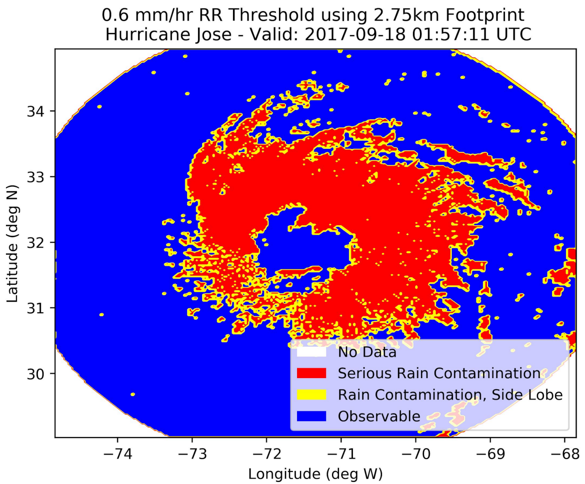

4.125 km Footprint

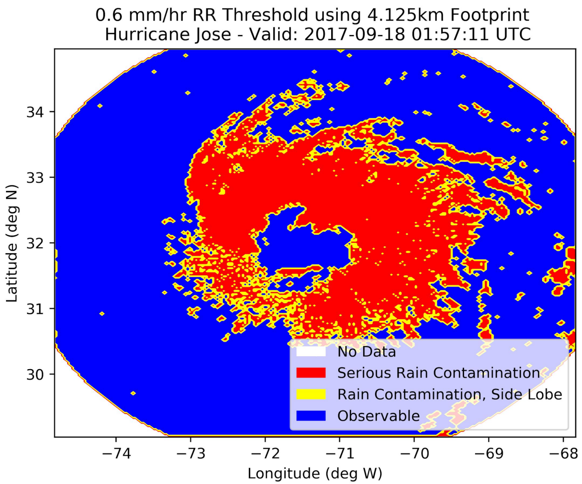

5.5 km Footprint

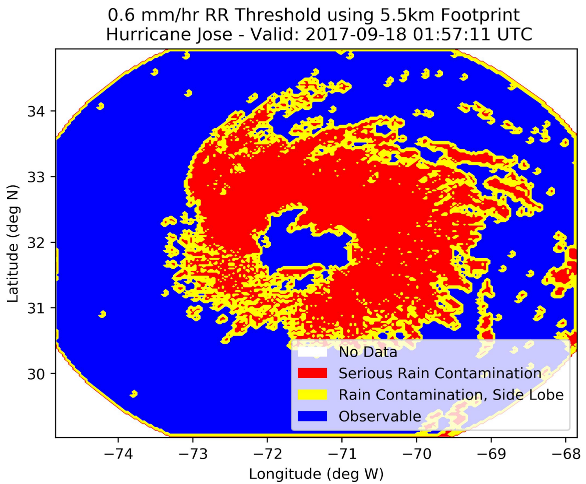

0.6 mm / hr rainrate threshold applied to reflectivity data for Jose (September 18th, 2017 1:57:11 UTC) with three shades:
blue: rainrate threshold met *and* surface observable
yellow: rainrate threshold met but surface *not* observable,
red: rainrate threshold not met *and* surface not observable

8.0 mm/hr Threshold (C-Band)

2.75 km Footprint

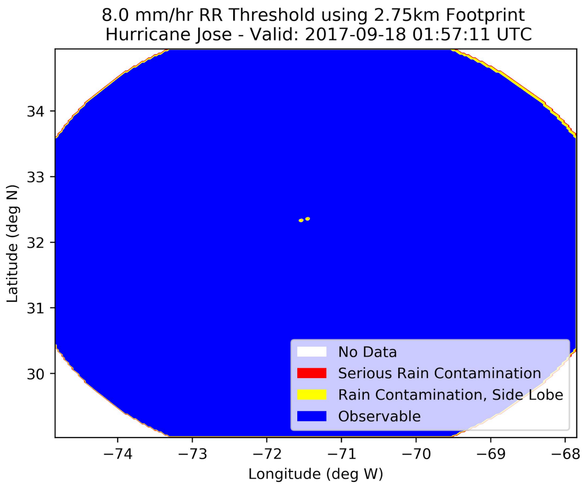

4.125 km Footprint

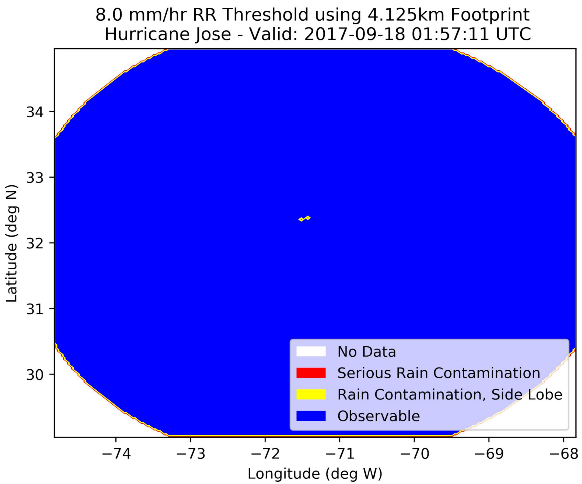

5.5 km Footprint

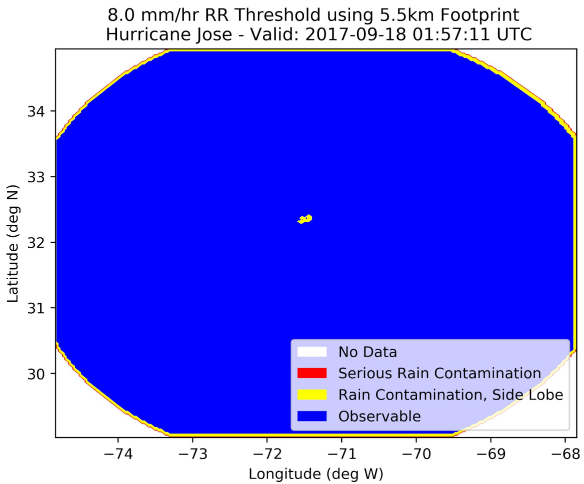

8.0 mm / hr rainrate threshold applied to reflectivity data for Jose (September 18th, 2017 1:57:11 UTC) with three shades:

blue: rainrate threshold met *and* surface observable

yellow: rainrate threshold met but surface *not* observable,

red: rainrate threshold not met *and* surface not observable

Rain Contamination Assessment

Percentage of Rain Contamination (Serious and Side Lobe) using 2.75 km Footprint.

Storm	Ka-Band (%)	Ku-Band (%)	C-Band (%)
Harvey	38.581414	16.802261	0.162331
Irma	29.070700	11.328826	0.196707
Jose	38.411000	22.161955	0.003819
Maria	34.110363	13.342632	0.017196
Nate	27.912528	12.463712	0.042016

Percentage of Rain Contamination (Serious and Side Lobe) using 5.5 km Footprint.

Storm	Ka-Band (%)	Ku-Band (%)	C-Band (%)
Harvey	49.448073	26.607081	1.455253
Irma	36.929452	16.468049	1.388411
Jose	45.859434	29.893048	0.928189
Maria	42.825206	20.779195	0.970651
Nate	35.166157	17.910618	1.048510

Percentage of Rain Contamination (Serious and Side Lobe) using 8.25 km Footprint.

Storm	Ka-Band (%)	Ku-Band (%)	C-Band (%)
Harvey	51.974714	28.971391	2.127497
Irma	39.058859	18.156296	2.033917
Jose	47.729182	31.860198	1.478227
Maria	45.089422	22.896285	1.534316
Nate	37.226890	19.619938	1.629106

Percentage of Rain Contamination (Serious and Side Lobe) using 11.0 km Footprint.

Storm	Ka-Band (%)	Ku-Band (%)	C-Band (%)
Harvey	61.678316	37.254115	4.096482
Irma	47.387418	24.137733	3.697337
Jose	54.436592	38.294499	2.759740
Maria	53.691531	30.157062	2.875649
Nate	45.261650	25.412528	3.048128

Conclusions

OBJECTIVE: Determine characteristics that improve present WaCM satellite technologies

- Largest 5.5 km footprint does provide sufficient rain-free coverage in the eye to make practical conclusions about intensity changes, but substantially more coverage would occur with smaller footprints

- Control variables (rainrate threshold, footprint size, case study) *independent* of TC structure

- Ideal parameters: > 0.6 mm/hr threshold, footprint size < 4.125 km, highly sheared system
    - Compromise between spatial resolution and penetrating power given current technologies
    - Produced least sensitivity to aforementioned biases
    - More power with smaller footprints
    - Big antenna and longer wavelength (C-band) are preferred for hurricane wind research, though it is more expensive to achieve the desired resolution at such wavelengths

QUESTIONS

Acknowledgements:

This undergraduate research assistantship was supported by NOAA's Global Ocean Monitoring and Observing Program via the Northern Gulf of Mexico Cooperative Institute managed by Mississippi State University. I would also like to thank the Hurricane Research Division/AOML for granting access to LF and TDR radar data, Risk Management Solutions HWind for access to their QC Application, operational data platforms, and HWind database to construct historical reanalysis snapshots. A special thanks is also given to his committee members, Drs. Mark Bourassa, Heather Holbach, Vasubandhu Misra, and Monica Hurdal, as well as the Marine Data Center research team at COAPS for assistance in all elements of this project.

References

Barnes, C. E., and G. M. Barnes, 2014: Eye and eyewall traits as determined with the NOAA WP-3D lower-fuselage radar. *Mon. Wea. Rev.*, **142**, 3393-3417, doi: 10.1175/MWR-D-13-00375.1

Barnes, G. M., E. J. Zipser, D. Jorgensen, and F. Marks, Jr., 1983: Mesoscale and Convective Structure of a Hurricane Rainband. *J. Atmos. Sci.*, **40**, 2125-2137, doi:10.1175/1520-0469%281983%29040<2125%3AMACSOA>2.0.CO%3B2

Barnes, G. M., and G. J. Stossmeister, 1986: The Structure and Decay of a Rainband in Hurricane Irene (1981). *Mon. Wea. Rev.*, **114**, 2590-2601, doi: 10.1175/1520-0493%281986%29114<2590%3ATSADOA>2.0.CO%3B2

Bourassa, M. A., E. Rodriguez, and D. Chelton, 15 July 2016: Winds and currents mission: Ability to observe mesoscale AIR/SEA coupling. *2016 IEEE International Geoscience and Remote Sensing Symposium (IGARSS)*, Beijing, 2016, 7392-7395, doi: 10.1109/IGARSS.2016.7730928

Bourassa, M. A., and Coauthors, 2019: Remotely sensed winds and wind stresses for marine forecasting and ocean modeling. *Front. Mar. Sci.,* **6**, 1-28, doi: 10.3389/fmars.2019.00443

Hurricane Research Division - Atlantic Oceanographic & Meteorological Laboratory, 2019: Radar lower fuselage sweep format. Accessed 21 October 2019, https://www.aoml.noaa.gov/hrd/format/lfsweepfileformat.html

Kepert, J.D., 2018: The boundary layer dynamics of tropical cyclone rainbands. *J. Atmos. Sci.,* **75**, 3777–3795, doi: 10.1175/JAS-D-18-0133.1

Marks, F. D., 1985: Evolution of the Structure of Precipitation in Hurricane Allen (1980). *Mon. Wea. Rev.*, **113**, 909-930, doi: 10.1175/1520-0493(1985)113<0909:EOTSOP>2.0.CO;2

Rodriguez, E., M. Bourassa, D. Chelton, J. T. Farrar, D. Long, D. Perkovic-Martin, and Roger Samelson, 2019: The Winds and Currents Mission Concept. *Front. Mar. Sci.*, **6**, 1-8, doi: 10.3389/fmars/2019.00438

Senn, H.V. and H.W. Hiser, 1959: On the Origin of hurricane spiral rainbands. *J. Meteor.*, **16**, 419–426, doi: 10.1175/1520-0469(1959)016<0419:OTOOHS>2.0.CO;2

Skwira, G. D., J. L. Schroeder, and R. E. Peterson, 2005: Surface Observations of Landfalling Hurricane Rainbands. *Mon. Wea. Rev.*, 133, 454-465, doi: 10.1175/MWR-2866.1

Stephens, G.L. and C.D. Kummerow, 2007: The Remote Sensing of Clouds and Precipitation from Space: A Review. *J. Atmos. Sci.*, **64**, 3742–3765, doi: 10.1175/2006 JAS2375.1

Sitkowski, M., J. P. Kossin, and C. M. Rozoff, 2011: Intensity and Structural Changes during Eyewall Replacement Cycles. *Mon. Wea. Rev.*, **139**, 3829-3847, doi: 10.1175/MWR-D-11-00034.1

Uhlhorn, E.W. and P.G. Black, 2003: Verification of Remotely Sensed Sea Surface Winds in Hurricanes. *J. Atmos. Oceanic Technol.,* **20**, 99–116, doi: 10.1175/1520-0426(2003)020<0099:VORSSS>2.0.CO;2